2023 IEEE International Conference on Robotics and Automation (ICRA 2023)
May 29 - June 2, 2023. London, UK

Heading for the Abyss: Control Strategies for Exploiting Swinging of a Descending Tethered Aerial Robot

Max Polzin[1], Frank Centamori[1] and Josie Hughes[1]

***Abstract*— The use of aerial vehicles for exploration and data collection has the potential to significantly aid environmental monitoring in environments which are dangerous and hard to navigate. However, within these environments navigation can often be restricted by overhangs which are challenging to navigate, particularly so with the high payloads required for environmental monitoring. We propose utilizing a tethered bicopter with horizontal propellers. This spherical pendulum like system can exploit the tether, not only as a means of powering and recovering the robot, but also to assist its motion, i.e. by swinging to increase the workspace of the robot. Using PD-based control, we demonstrate how the system can be stabilized and bang-bang control to excite the system to achieve large amplitude swinging. By combining these controllers, we show how the system can be used to navigate in a glacial-inspired scenario where there are overhangs and obstacles through which the robot must navigate.**

I. Introduction

Flying robots and drones can demonstrate significant maneuverability, allowing for high-speed and precise motions to be performed. These capabilities have been utilized to develop flying robots which can assist with search and rescue scenarios, provide sensory data capture for agriculture domains, or even provide manipulation capabilities [1]. Environmental monitoring and exploration is one area where drones have significant potential [2], [3]. One particularly challenging case is the monitoring of extreme environments such as within glacial crevasses or moulins [4], [5]. These are extremely dangerous situations in which aerial robots could assist in monitoring and data-collection, reducing the risk to human field-scientists and allowing more frequent data sampling. However, there are a number of domain specific problems; large payloads can be required, the environment can be hazardous and have a complex structure, e.g. overhanging rocks or icicles [6]. These challenges can mean typical drone technologies are not best suited, in particular so for sustaining the movement of heavy monitoring or imaging equipment.

Tethered robotic systems have been shown to have many advantages in different domains, e.g. for locomotion in extreme environments [7], underwater exploration [8], or power generation [9]. Besides a reliable power and communication channel, tethers provide a mean of assisting or recovering the system. Utilizing tethers for drones could provide similar advantages. They can provide a physical constraint and ability to limit or control the motion of a robot. Further, tethers can allow for heavier loads to be flown. A number of tethered drones have already been shown including [10] and [11]. In [10] the tether is used to estimate an aerial vehicle's position where a swarm of tethered aerial vehicles is considered in [11]. In both cases, the tether is not considered to be taut, introducing a risk of entanglement, neither is the tether leveraged to provide physical advantages to the robot. The authors of [12] and [13] introduce controllers for tethered aerial vehicles. However, in both works a tether is assumed to be connected below the aerial vehicle and the aerial vehicle flies above an anchor point on the ground.

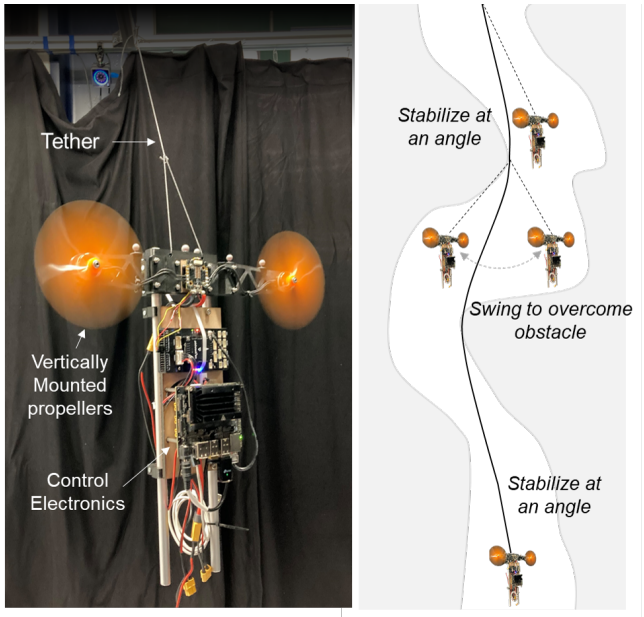

Fig. 1. Left: The proposed tethered bicopter design with horizontal propellers. Right: The tethered bicopter exploits dynamic swinging to descend and explore a glacial moulin.

An alternative approach is to utilize a flying robot with horizontal propellers, where the robot is suspended and hanging on the tether. The authors of [14] show the mass balance and capabilities of such an example system whereby the system is modeled as a double pendulum. The dynamics and control of propeller driven pendulum swinging in one plane with a rigid connection between anchor point and pendulum have been studied in [15]. The authors of [16] propose a bicopter design where propellers produce thrust perpendicular to the robot's tether. To further exploit propeller driven tethered robots, additional control approaches must be explored, in particular those that exploit the spherical pendulum like nature of such systems. We propose a novel tethered robot design with two horizontal propellers for

[1]The authors are with Faculty of Mechanical Engineering, Swiss Federal Institute of Technology Lausanne, 1015 Lausanne, Switzerland max.polzin@epfl.ch

deployment and monitoring in harsh conditions.

The proposed robot is well suited for use in extreme environments, e.g. glacial moulins or cave exploration, as the horizontal propellers are less susceptible to ice or debris falling from above. To prevent collisions in these unknown environments, it is possible to shield the propellers. The hanging nature of the robot ensures constant tension in the tether and allows the workspace to be actively controlled through the tether length.

The specific arrangement of the presented robot's components, i.e. the center of gravity being below the thrusters and the robots body being short compared to the tether length, allows expressing the robots dynamics as a simple pendulum.

By exploiting model-free PD-based control, we seek to explore how simple control policies can be used to stabilize the robot around the workspace. To explore how high payloads, e.g. environmental monitoring equipment weighing 4kg or more, could be carried or deployed within the environment, we propose a number of controllers that exploit the bodies pendulum dynamics to expand the workspace of the robot.

The contributions of this paper are threefold:

- We propose a novel tethered bicopter with horizontal propellers, where the design simplifies control and allows the addition of automatically stabilized sensor payloads.
- We describe the dynamics of the proposed tethered bicopter and introduce novel control schemes to stabilize it, to navigate on a cone and present operational stability constraints.
- We exploit the dynamics of the system and the proposed control algorithms to reach targets outside of the robot's stable area of operation.

II. Methods

In this section, we first describe the presented robot, a tethered bicopter with horizontal propellers. The equations of motion for such robots are then derived, after which we introduce a control scheme that allows for stabilization of the robot, and can exploit the dynamical behavior through swinging.

A. System description

Fig. 2 shows the tethered bicopter with horizontal propellers. The propellers are mounted symmetrically at a distance d from the center. They generate a thrust, F_l, and F_r, respectively. The fixed end of a tether is connected to an anchor point above the robot while the other end is connected to robot directly in the middle of the two propellers. The robot's body has height, h, and mass, m, whereby the center of mass is located below the propellers when the robot hangs. An inertial coordinate system located at the anchor is used to express the robot's position and orientation. The position of the robot, with respect to the anchor point is described by the length of the tether, l, and the angles, ϕ and θ, whereby θ and ϕ describe the inclination of the tether with respect to the vertical axis and the orientation of the tether in the horizontal plane. Finally, the angle, ψ, describes the free

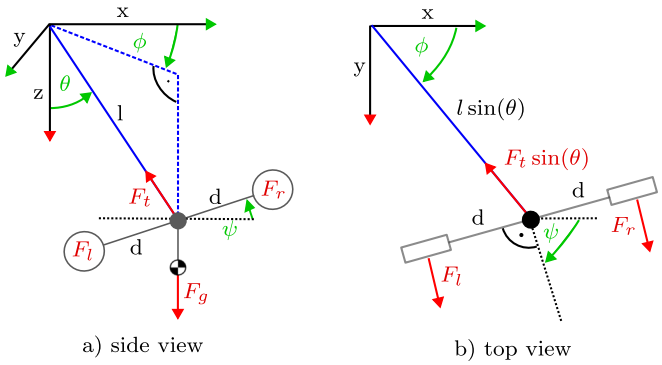

Fig. 2. Force diagram of the tethered bicopter robot in a) the side view and b) the top view. The inertial frame is located at the anchor point of the tether. The tether of length, l, is connected to the robot.

rotation of the robot around its attachment to the tether in a horizontal plane. Thus, the angle, ψ, can be interpreted as the robot's yaw angle. Fig. 2 shows the tethered robot in the inertial coordinate frame, where the position, orientation and forces acting on the robot are indicated.

B. System modeling

For long tether lengths, $l >> h$, we assume the robot's body can be modeled as a point mass, m, to derive its kinematics. The position of the robot is given by:

$$\begin{aligned} x &= l\sin\theta\cos\phi \\ y &= l\sin\theta\sin\phi \\ z &= l\cos\theta \end{aligned} \tag{1}$$

To model the dynamics of the robot, the thrust generated by the left and right propellers, F_L and F_R, and the gravitational force, $F_g = mg$, are considered. F_L and F_R act in the horizontal plane as the horizontal propellers are rigidly attached above the center of gravity. Thus, they act on the rotation of the robot through $D_F = F_L - F_R$ and contribute to its forward movement with $S_F = F_L + F_R$. Using Euler-Lagrangian method, the system dynamics can be derived as:

$$\begin{aligned} \ddot{\theta} &= \dot{\phi}^2\sin\theta\cos\theta - \frac{g}{l}\sin\theta + \frac{S_f\cos(\theta)}{ml} \\ \ddot{\phi} &= \begin{cases} -\frac{S_f\sin\psi}{ml\sin\theta} - \frac{2\dot{\theta}\dot{\phi}}{\tan(\theta)} & \text{if } \theta \neq 0 \\ \ddot{\psi} & \text{if } \theta = 0 \end{cases} \\ \ddot{\psi} &= \frac{d}{I_\psi}D_F - \frac{GJ}{l}\psi \end{aligned} \tag{2}$$

When the angle θ is close to 0, both ϕ and ψ have the same dynamics, as rotation of the robot also change directly its orientation. Note, the torsion of the tether introduces a moment, which is given through the tethers' modulus of rigidity, G, and the torsional constant, J, of its material. For long tethers or when the tether is mounted such that its rotation is decoupled from the robot's body, its contribution to the system dynamics is negligible and therefore can be ignored.

With three degrees of freedom and only two thrusters, the system is underactuated. The deviation from vertical, θ, and

the robot's deviation from the ϕ-plane, ψ, are directly controllable by the sum and difference of the thrust, S_F, and D_F. However, the robot's position, ϕ, is coupled to both inputs, S_F and D_F. When the robot's thrusters are off, its dynamics simplify to those of a spherical pendulum. Maintaining stable flight behavior and avoiding loss of balance requires active control of the robot.

C. Controller design

A control scheme to set the robot's heading angle, ψ, and its deviation from the vertical, θ, is proposed. It is shown, that by controlling ψ and θ, the robot stabilizes as well in ϕ. The deviation of the robot from the vertical axis, θ, is directly linked to the sum of the input thrusts, S_F. Control inputs, u_θ, correspond to a percentage of throttle command for left and right thruster. They map to the sum of thrust by a non-linear function

$$S_f = f(u_\theta) \quad \text{with} \quad S_f \in \left[S_{f,min}, S_{f,max}\right] \tag{3}$$

and cause the robot to stabilize at:

$$\theta^* = \arctan\left(\frac{S_f}{F_g}\right). \tag{4}$$

The robot's heading angle, ψ, can be controlled using a feedback controller,

$$u_\psi = \mathrm{PD}(\psi^* - \hat{\psi}), \tag{5}$$

where ψ^* is the setpoint angle and $\hat{\psi}$ is the estimated heading angle. The gains of the PD controller depend on the robot's inertia and can be set accordingly.

The percentage of throttle setpoints of the two propellers can therefore be given as a function of u_θ and u_ψ:

$$\begin{aligned} u_{\text{left}} &= \frac{u_\theta}{2} + u_\psi \\ u_{\text{right}} &= \frac{u_\theta}{2} - u_\psi. \end{aligned} \tag{6}$$

For setpoints, ψ^* and θ^*, the robot stabilizes automatically at $\phi = \psi^*$ and thus it stabilizes in θ, ϕ, and ψ.

1) Moving around the cone: In order to move from one point, θ_0, ϕ_0, ψ_0, to another point θ_1, ϕ_1, ψ_1, a trajectory controller is introduced to linearly interpolate between the two setpoints and apply intermediate steps, $\Delta\theta, \Delta\phi, \Delta\psi$, such that the system does not loose stability. For a constant input thrust, $S_f = \text{constant}$, the robot's operational range is described by a cone.

2) Swinging: For stable flight the operational range of the robot is limited by

$$\theta_{max} = \arctan\left(\frac{S_{f,max}}{F_g}\right) \tag{7}$$

However, it can be extended by exploiting the robot's pendulum dynamics. When the robot faces direction, ϕ, the period of the natural frequency of the system is given by

$$T = 2\pi\sqrt{\frac{l}{g}} \tag{8}$$

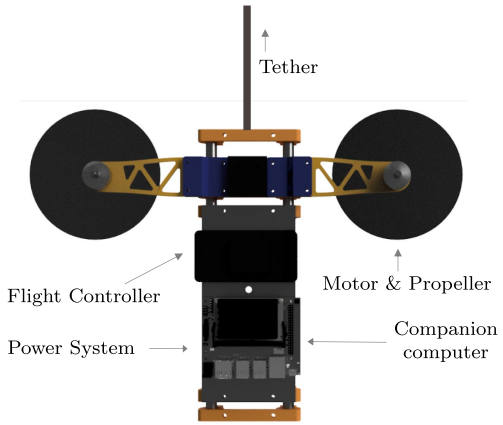

Fig. 3. The two propellers are located left and right of the robot's middle. The tether lead-out is centered at the robot's top. Payload, power management system, motor and flight controller and companion computer are mounted below the propellers.

Note, the natural frequency is independent of the robot's mass and hence its payload. Two control schemes are proposed to excite the system at its natural frequency to build up momentum to extend the operational range.

a) Bang-bang thrust control: To excite the robot at its natural frequency, the input thrust, S_f, can be set to be periodic, in the form of:

$$S_f = \begin{cases} S_{f,max} & \text{for } t < T/2 \\ S_{f,min} & \text{for } T/2 < t < T \end{cases} \tag{9}$$

where the heading angle, ψ^*, is kept constant. This results in the robot swinging forward and backward gradually building up momentum. Note, in this control scheme the robot always faces into the same direction, ϕ.

b) Bang-bang ψ control: In a second and contrasting controller the robot is excited with a constant thrust, S_f, and its commanded heading angle, ψ^*, has a periodic form of:

$$\psi* = \begin{cases} \phi & \text{for } 0 \le t < T/2 \\ -\phi & \text{for } T/2 \le t < T \end{cases} \tag{10}$$

Under this control scheme the robot is swinging in the ϕ-plane. After reaching the highest point in the swinging motion it performs half a turn. Note, according to (3), the robot will only fly stable in the ϕ-plane,if it turns fast enough at the peak points, i.e. $\psi = \pm\pi$.

D. Experimental setup

Fig. 3 shows the mechanical setup of the tethered bicopter. It is constructed from two vertical aluminum beams which are linked by 3D-printed connectors. The two propellers, the system's power management system, the flight controller and companion computer are mounted to the extendable aluminum beams. The robot weighs approximately 1kg. Two brushless DC motors drive the propellers. The motors are controlled via a Foxeer Reaper Mini Electronic Speed Controller which receives commands from a Holybro Pixhawk 6X flight controller that runs a modified PX4 firmware, see [17]. The PX4 flight stack implements an Extended

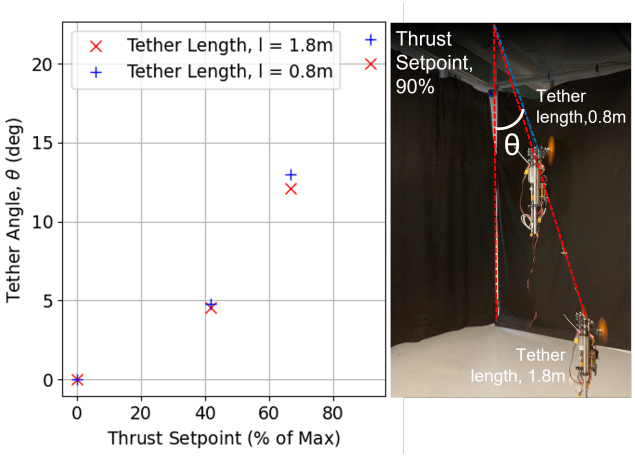

Fig. 4. The maximum tether angle that is measured for different thrust setpoints for two different lengths of tether, $l = 1.8m$ and $l = 0.8m$.

Kalman Filter which estimates the vehicles attitude, i.e. its heading angle, $\hat{\psi}$. Further, it provides information about the system's power status. The Pixhawk 6X flight controller is connected via Ethernet to an onboard companion computer. The onboard companion computer is a Nvidia Jetson Nano. The companion computer implements a web-based user interface and the control algorithms to achieve stable flight and swinging motion using ROS 2, [18]. Control algorithms transmit data at 100Hz. Sensor measurements, system statistics and user inputs are transmitted via WiFi from the companion computer to a ground station.

III. Experimental Results

In this section experimental results are presented that showcase the performance of the controllers and the demonstration of their use. First, it is shown that the robot can achieves stable flight for varying θ setpoints with different thrust inputs. Second, it is shown that the robot can move stable on a cone if the rate of turn is selected appropriately. Comparison of the swinging controllers of the swinging controllers and their resulting dynamic behaviors are then explored. Finally, it is demonstrated how the robot can exploit swinging to extend its operational range.

A. Moving out of the vertical

The proposed robot is capable to achieve stable deviation from the vertical for different tether lengths. The robot starts hanging at $\theta = 0$ below its anchor point. Initially, the thrust is set to 0, which is then increased to 0.9 of the maximum thrust. In response, the robot deviates from the vertical and θ gradually increases. Eventually, the robot stabilizes at

$$\theta_{0.9} = \arctan\left(\frac{S_{f,0.9}}{F_g}\right). \tag{11}$$

Fig. 4 shows how the robot converges for two tether lengths, $l_1 = 0.9$, and $l_2 = 1.8$, with the robots position recorded using an Optitrack motion capture system. The system is stable in ϕ-direction. For the longer tether length, l_2, $\theta_{0.9}$ is slightly slower than for the shorter tether length. We believe this results from the center of mass being below the tether attachment point such that the system could be considered as a double-pendulum. Further work is required to better explore this effect.

B. Moving around on a cone

If the robot flies at a constant angle θ^*, and the yaw setpoint, ψ^*, is varied, the robot will change its ϕ position and eventually stabilize at $\psi = 0$. However, if the robot changes its heading angle to quickly, it will severely increase the duration until the robot stabilizes. In this experiment, the robot starts with a constant angle, θ, and is commanded to turn 180 degrees. The trajectory controller limits $\Delta\psi$. Depending on the step size of $\Delta\psi$, the robot requires different times to complete a 180 degree turn. Fig. 5 shows the position of the robot as it performs a 180 degree turn and stabilizes for three different controller rates and two tether lengths. Note, the gains of the PD-controller to stabilize in the yaw direction are constant across all trials. For lower $\Delta\psi$, the robot describes an arc for both tether lengths. When $\Delta\psi$ is too large, i.e. the turning period is too short, the robot looses balance and requires a long time to stabilize. This is clearly seen by the 1s duration turns, which result in significant oscillations after making the 180 degree turn.

C. Swinging

The two proposed swinging controllers are evaluated while the robot caries payloads between 0kg and 4kg. The robot starts with no thrust hanging below its anchor point. In each experiment, the deployed controller either commands varying thrust or yaw commands to the robot. Both controllers create a swinging motion. The thrust varying controller keeps the robot facing forward, while the yaw varying controller turns the robot 180 degrees when it reaches its limits on either side of the swing. Fig. 6 shows the robot's trajectories recorded with a motion tracking system.

For the thrust varying controller, the robot is swinging smoother back and forth than for the yaw varying controller. However, small perturbations in the robot's heading angle when swinging backwards with no thrust, lead to a gradual change in the robot's ϕ angle. With no load the robot requires eleven periods until it reaches the maximum swinging angle, $x_{max} = 1.05$m. After eleven periods the aerodynamic drag of the robot is too high to increase its swinging distance any further. For payloads of 2kg and 4kg, the robot reaches $x_{11} = 0.4$ and $x_{11} = 0.3$ after eleven periods and will reach lower maximum distances of $x_{max} = 0.8$m and respectively $x_{max} = 0.7$m after 25 and 34 periods respectively.

The yaw varying controller is reaching a maximum swinging distance, $x_{max} = 1.2$, after just six periods. For payloads of 2kg and 4kg it reaches similar distances. The alternating turning direction of the robot reduces the robot's deviation for higher payloads. For no payload, the robot's yaw angle does not stabilize fast enough and it leads to more chaotic flight behavior. Note, for the yaw varying controller the robot has reached greater swinging distances after six periods than the thrust varying controller. The thrust varying controller requires approximately two times more excitation periods

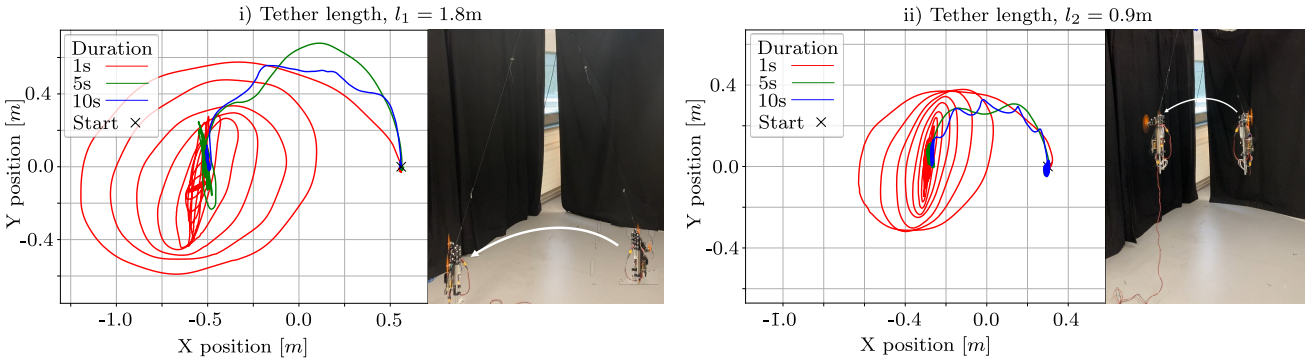

Fig. 5. The robot is commanded to turn 180 degrees. The underlying controller limits its turning speed. The left figure shows the robots trajectory for a tether length of 1.8m, the left one for 0.9m. If the robot moves too fast, e.g. completes a turn in one second, it looses balance and requires a long time to stabilize at its new position.

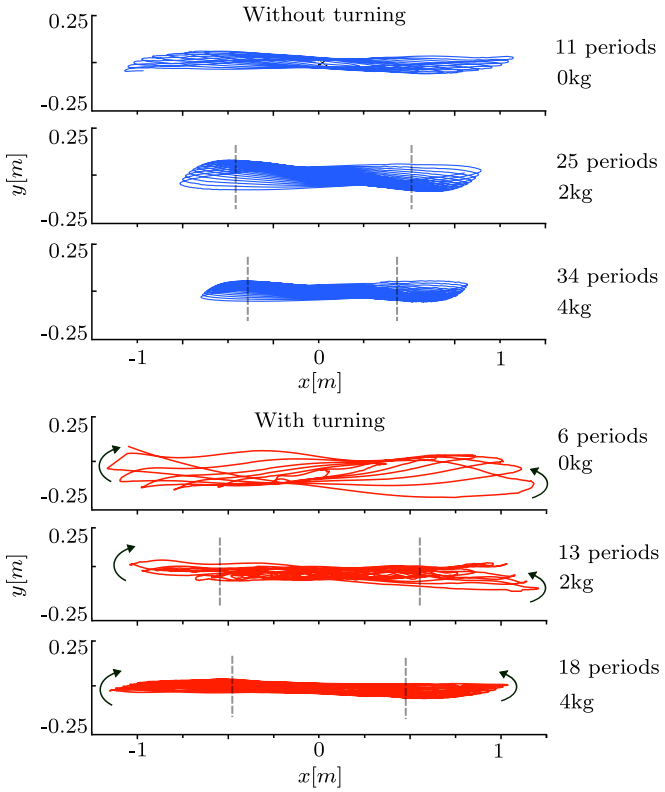

Fig. 6. For the two control strategies (with and without turning) the distance moved in the x axis is shown until steady state swinging is achieved. This is performed for different payloads, and the number of cycles to achieve this steady-sate swinging is shown.

to reach the maximum swinging distance than the yaw varying controller, while achieving lower maximum swinging distances for all payloads.

D. Demonstration

The proposed swinging controller can be used to increase the operational range of the presented tethered bicopter. Fig. 7 demonstrates how the tethered robot navigates around two obstacle to reach a target. The robot starts its descend close to its anchor point. It descends with a constant angle θ to navigate around a first obstacle. To overcome a second obstacle, the robot exploits its swinging dynamics. When reeling out the tether, the kinematic model's assumption of a constant tether length is violated. In practice, this does not affect the robot's ability to stabilize. Note, the robot can also be retracted using the same scheme.

IV. Discussion and Future Work

Developing robots for exploration of complex structures and terrains has the potential for significant impact in environmental research. Motivated by this, we investigated control approaches for a bicopter robot with horizontal propellers, which is suited for the exploration of extreme terrain, and has the capabilities to carry high payloads. We propose control approaches which use only IMU data from the robot, and leverage both stabilization and swinging to navigate around obstacles and explore structures with overhangs. The robot's potential to explore complex natural environments is shown in laboratory demonstrations.

Although the demonstrated PD-controller allows for control of the robot, and the gains can be tuned to prevent notable overshoot, further work to improve the autonomy and stabilization of the underactuated robot should be explored. To develop improved controllers additional sensors are required, e.g. measurements of the tether angle or a localization method based on LiDAR or visual measurements. Combining additional sensor measurements with a model of the thrusters and the system dynamics would allow the application of Model Predictive Control (MPC) to be explored. Different control methods could be evaluated in simulation.

Finally, to assess the robot's control and application capabilities, it could be rappelled into a glacial moulin for exploration and to gather data. In addition, this would advance glacial research, where to date, there has only been manual exploration. Here it would be possible to compare and contrast the performance to a drone, to quantify the advantages in terms of payload, maneuverability, stability and usability.

References

[1] M. Hassanalian and A. Abdelkefi, "Classifications, applications, and design challenges of drones: A review," *Progress in Aerospace Sciences*, vol. 91, pp. 99–131, 2017.

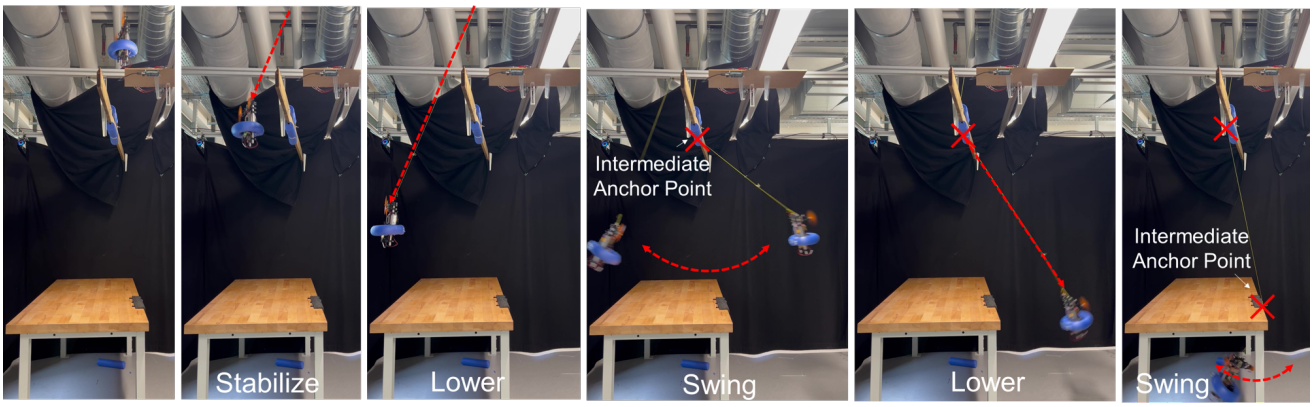

Fig. 7. Demonstration of utilizing stabilization and swinging to descend into spaces with under and over hangs. The robot utilizes different controllers to overcome obstacles and forming intermediate anchor points.

[2] G. Rohi, O. Ejofodomi, and G. Ofualagba, "Autonomous monitoring, analysis, and countering of air pollution using environmental drones," en, *Heliyon*, vol. 6, no. 1, e03252, Jan. 2020.

[3] J. Paneque-Gálvez, M. K. McCall, B. M. Napoletano, S. A. Wich, and L. P. Koh, "Small drones for community-based forest monitoring: An assessment of their feasibility and potential in tropical areas," *Forests*, vol. 5, no. 6, pp. 1481–1507, 2014.

[4] W. Fink, M. Tarbell, R. Furfaro, and J. Kargel, "Tier-scalable reconnaissance missions for autonomous exploration and spatio-temporal monitoring of climate change with particular application to glaciers and their environs," in *AGU Fall Meeting Abstracts*, vol. 2010, 2010, NH52A–08.

[5] A. Bhardwaj, L. Sam, S. Singh, and R. Kumar, "Automated detection and temporal monitoring of crevasses using remote sensing and their implications for glacier dynamics," *Annals of Glaciology*, vol. 57, no. 71, pp. 81–91, 2016.

[6] J. Vallot, "Exploration des moulins de la mer de glace," *Collections de glaciologie*, vol. 3, no. 1, pp. 183–193, 1898.

[7] P. McGarey, M. Polzin, and T. D. Barfoot, "Falling in line: Visual route following on extreme terrain for a tethered mobile robot," in *2017 IEEE International Conference on Robotics and Automation (ICRA)*, May 2017, pp. 2027–2034.

[8] E. C and G. Moses, "Prototype development of tethered underwater robot for underwater vessel anchor release," *IAES International Journal of Robotics and Automation (IJRA)*, vol. 9, Sep. 2020.

[9] T. A. Wood, H. Hesse, M. Polzin, E. Ahbe, and R. S. Smith, "Modeling, identification, estimation and adaptation for the control of power-generating kites," *IFAC-PapersOnLine*, vol. 51, no. 15, pp. 981–989, 2018, Publisher: Elsevier.

[10] S. Kiribayashi, K. Yakushigawa, and K. Nagatani, "Position estimation of tethered micro unmanned aerial vehicle by observing the slack tether," in *IEEE International Symposium on Safety, Security and Rescue Robotics (SSRR)*, Oct. 2017, pp. 159–165.

[11] M. Bolognini and L. Fagiano, "LiDAR-Based Navigation of Tethered Drone Formations in an Unknown Environment," en, *IFAC-PapersOnLine*, 21st IFAC World Congress, vol. 53, no. 2, pp. 9426–9431, Jan. 2020.

[12] S. Lupashin and R. D'Andrea, "Stabilization of a flying vehicle on a taut tether using inertial sensing," in *2013 IEEE/RSJ International Conference on Intelligent Robots and Systems*, Nov. 2013, pp. 2432–2438.

[13] M. M. Nicotra, R. Naldi, and E. Garone, "Taut Cable Control of a Tethered UAV," en, *IFAC Proceedings Volumes*, 19th IFAC World Congress, vol. 47, no. 3, pp. 3190–3195, Jan. 2014.

[14] P. J. McKerrow and D. Ratner, "The design of a tethered aerial robot," in *Proceedings 2007 IEEE International Conference on Robotics and Automation*, ISSN: 1050-4729, Apr. 2007, pp. 355–360.

[15] M. M. Job and P. Subha Hency Jose, "Modeling and control of mechatronic aeropendulum," in *2015 International Conference on Innovations in Information, Embedded and Communication Systems (ICIIECS)*, Mar. 2015, pp. 1–5.

[16] S. Kirchgeorg and S. Mintchev, "Multimodal aerial-tethered robot for tree canopy exploration," in *2022 IEEE/RSJ International Conference on Intelligent Robots and Systems (IROS)*, Kyoto, Japan: IEEE, Oct. 2022, pp. 6080–6086.

[17] L. Meier, D. Honegger, and M. Pollefeys, "PX4: A node-based multithreaded open source robotics framework for deeply embedded platforms," in *2015 IEEE International Conference on Robotics and Automation (ICRA)*, May 2015, pp. 6235–6240.

[18] S. Macenski, T. Foote, B. Gerkey, C. Lalancette, and W. Woodall, "Robot Operating System 2: Design, architecture, and uses in the wild," *Science Robotics*, vol. 7, no. 66, eabm6074, May 2022, Publisher: American Association for the Advancement of Science.